Gluing Torus Families across a Singularity: The Lens Space for the Hydrogen Atom in Crossed Fields

Thomas Bartsch,[1] Stephan Gekle,[2] Jörg Main[3] and Turgay Uzer[4]

[1]*Department of Mathematical Sciences, Loughborough University, Loughborough LE11 3TU, UK*
[2]*Department of Applied Physics, University of Twente, 7500 AE Enschede, The Netherlands*
[3]*Institut für Theoretische Physik I, Universität Stuttgart, 70550 Stuttgart, Germany*
[4]*Center for Nonlinear Science, School of Physics, Georgia Institute of Technology, Atlanta, GA 30332-0430, USA*

We demonstrate that topological information that can be extracted from periodic orbits in a near-integrable system can lead to a complete topological characterization of families of invariant 2-tori in terms of lens spaces. This approach ties in with the techniques we developed for classifying the tori in systems with more than two degrees of freedom. It therefore offers a general way to investigate families of invariant 2-tori in higher-dimensional Hamiltonian systems.

§1. Introduction

Periodic orbits are the simplest invariant objects in the phase space of a dynamical system.[1)] Because they form the fundamental building blocks of the dynamics and because they are much simpler to calculate numerically than any more complicated structures, they are widely used as a tool to study the geometrical and dynamical structure of a multidimensional phase space.[2),3)] In a near-integrable system, the phase-space structure is dominated by a hierarchy of invariant tori of various dimensions. As we showed in a recent series of publications,[4)] the existence of such a hierarchy, about which no detailed knowledge is required, can be used to impose an ordering principle upon the periodic orbits, and conversely, this ordering of periodic orbits allows one to obtain information about the higher-dimensional invariant tori that are not easily accessible through direct numerical methods.

In the present paper we will demonstrate how the results of our earlier work can be extended into a complete topological characterization of families of invariant tori. Since we found the familiar Poincaré surface of section plots a somewhat unreliable tool to this end, we will analyze the singularities of Poincaré maps that lead to this failure, and we will show how the nature of the singularities is related to the topology of the family of tori under consideration.

Because the present paper is focused on the topology of families of 2-tori, which exist in systems with two or more degrees of freedom, and on their representation in Poincaré plots, which are available only in two degrees of freedom, we will largely restrict our discussion to this case. Nevertheless, we will also show how these results can be generalized to higher-dimensional systems.

The outline of the paper is as follows: In §2 we briefly review the properties of

Hamiltonian systems that we will need. Sections 3 and 4 describe the invariant tori in two example systems, namely the crossed-fields hydrogen atom (following Ref. 4)) and the two-dimensional harmonic oscillator. Section 5 outlines the theory of lens spaces that we need to carry out the topological classification of the families of tori, which we do in §6.

§2. Phase space structures in Hamiltonian systems

Among all Hamiltonian systems, integrable systems exhibit the most regular dynamics. By definition, a system with two degrees of freedom is integrable if it possesses a constant of motion independent of the Hamiltonian. The regular level sets of these constants are 2-dimensional tori if they are compact.[5),6)] In an integrable system, action-angle variables ($\boldsymbol{I}$, $\boldsymbol{\varphi}$) can be introduced such that (i) the action variables $\boldsymbol{I}$ are constants of motion and characterize the invariant tori, (ii) the angles $\boldsymbol{\varphi}$ determine the position on an individual torus, and they increase linearly with time

$$\boldsymbol{\varphi}(t) = \boldsymbol{\omega} t + \boldsymbol{\varphi_0} \,, \tag{1}$$

with a constant frequency vector $\boldsymbol{\omega}(\boldsymbol{I})$ and initial conditions $\boldsymbol{\varphi_0}$. If the ratio of the frequencies on a torus is rational,

$$\omega_1/\omega_2 = w_1/w_2 \,, \tag{2}$$

that torus is called resonant. It carries periodic orbits (POs), and the integer winding numbers w_i specify how often the angle φ_i runs though the range from 0 to 2π before the POs repeat themselves.

Angle coordinates $\boldsymbol{\varphi}$ on a given torus can be defined in various ways.[7)] Apart from a choice of origin, which is inconsequential, any two angle coordinate systems are related by a linear transformation

$$\boldsymbol{\varphi'} = M \cdot \boldsymbol{\varphi} \,, \tag{3}$$

where M is a 2×2 integer matrix with $\det M = \pm 1$. The action coordinates must be transformed according to

$$\boldsymbol{I'} = (M^{\mathrm{T}})^{-1} \cdot \boldsymbol{I} \,, \tag{4}$$

whereas the winding numbers on a rational torus transform as the angles in Eq. (3).

In a non-integrable system, a resonant torus breaks up into isolated POs.[5),8)] According to Kolmogorov-Arnold-Moser (KAM) theory,[5),9)] most nonresonant tori remain intact in a near-integrable system and break up only gradually. They are interspersed with the isolated POs in the same way as resonant and nonresonant tori are interspersed in the integrable limit. Therefore, POs can be used to investigate the structure of both the surviving tori in the perturbed system and the continuous family of invariant tori in the integrable limit. Because of this close connection between POs and invariant tori, and for simplicity of expression, we will not always distinguish between broken and surviving tori. We will usually speak of the invariant tori as if they occurred in a continuous family even in the non-integrable setting, keeping in mind that we gain information on this family only through the POs that arise from the breakup of the resonant tori.

§3. Invariant tori in the crossed-fields hydrogen atom

In this section, we will briefly summarize the key facts concerning the POs and invariant tori in the crossed-fields hydrogen atom that were obtained in Ref. 4), to which the reader is referred for further details. Although the focus of Ref. 4) is the development of computational tools that allow one to characterize the topology of invariant tori in systems with more than two degrees of freedom, here we will restrict our discussion, for simplicity, to a two-degree-of-freedom subsystem of the full three-dimensional dynamics, viz. the plane perpendicular to the magnetic field. As will be discussed briefly in §6, the results obtained here generalize immediately to the higher-dimensional setting of Ref. 4).

The electron motion in a hydrogen atom exposed to an electric field F in the x direction and a magnetic field B in the z direction is governed by the Hamiltonian,[10] in atomic units,

$$H_{\rm atom} = \frac{1}{2}\boldsymbol{p}^2 - \frac{1}{r} + \frac{B}{2}\left(p_y x - p_x y\right) + \frac{B^2}{8}\left(x^2 + y^2\right) - Fx \ , \tag{5}$$

where the position vector is $\boldsymbol{r} = (x, y)$, the conjugate momentum $\boldsymbol{p} = (p_x, p_y)$, and $r = \sqrt{x^2 + y^2}$. The dynamics described by the Hamiltonian (5) is integrable in the absence of external fields, i.e. for $B = 0$ and $F = 0$. Integrability is lost if $B > 0$. We will here treat the crossed-fields hydrogen atom in a parameter range where the phase space structure is dominated by the remnants of invariant tori. Nevertheless, the external fields are chosen too strong for perturbation theory to be a reliable tool, and we will consider the full nonintegrable Hamiltonian (5).

Our study of the crossed-fields system begins with a numerical search for POs. The resulting POs are represented in Fig. 1. The two shortest or fundamental periodic orbits (FPOs) are marked with S^+ and S^-, following the notation of Refs. 11) and 12). As can be clearly seen in the Poincaré surface of section plot

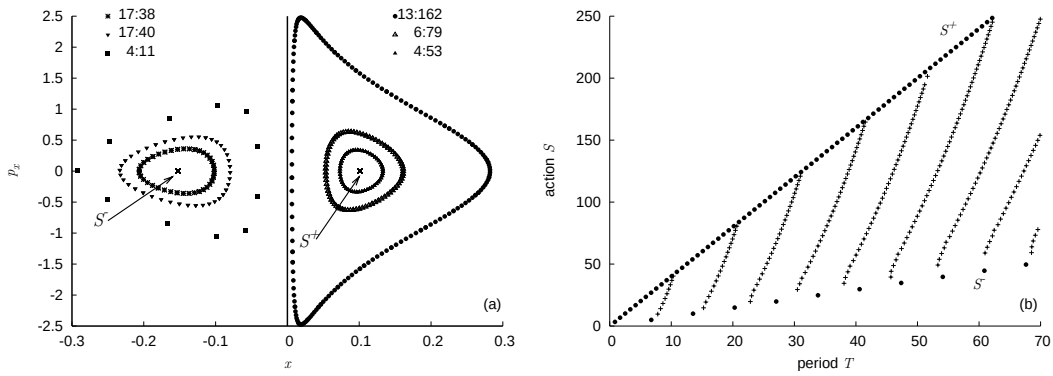

Fig. 1. Two representations of the POs in the planar crossed-fields hydrogen atom: (a) Poincaré surface of section plot $y = 0$. Non-fundamental POs are labeled with winding numbers transverse and longitudinal to the FPO around which they are centered. The vertical line at $x = 0$ indicates the location of the Coulomb singularity. (b) Periods and actions of the fundamental (circles) and non-fundamental (crossed) POs and their repetitions.

in Fig. 1(a), both FPOs are stable and are surrounded by families of invariant 2-tori (which we identify through the isolated POs embedded in them, as discussed above). In the terminology of Ref. 4), the FPOs serve as organizing centers for the POs surrounding them. The plot clearly exhibits *two* distinct families of 2-tori that are organized by the two FPOs and separated from each other by the Coulomb singularity at $x = 0$.

A very different view of the scenario is offered by Fig. 1(b), which displays the periods and actions of the POs. In this graph the FPOs S^+ and S^- and their two-, three-, and higher-fold repetitions appear on straight lines through the origin. The non-fundamental POs fall in series that begin and end at the lines formed by the FPOs. These series indicate that the POs should be regarded as forming a *single* family that stretches continuously from one FPO to the other and for which both FPOs serve as organizing centers. This interpretation is justified in more detail in Ref. 4).

When the continuous family of invariant tori is projected into a Poincaré surface of section, every torus appears as a closed curve surrounding one of the FPOs. On a planar surface it is impossible to achieve a continuous transition from curves that enclose S^- to those that enclose S^+. Therefore, a singularity must appear that separates the two half-families. In this case, the Coulomb singularity at $x = y = 0$ naturally serves this purpose. The appearance of the Poincaré plot can be reconciled with the existence of a single family if it is assumed that the two half-families are glued together, i.e. the outermost tori of the two half-families are identified. The topology of the total family is then determined by the way in which this identification is carried out. If it is possible, therefore, to specify the map through which the two boundary tori are identified, the topology of the family is known.

As described in Ref. 4), this can indeed be achieved by noting that each FPO imposes a specific system of angle coordinates upon the surrounding tori so that one "longitudinal" angle coordinate φ_l describes the motion along the FPO, the other coordinate φ_t the motion transverse to it. Through a careful analysis of the winding numbers associated with the POs in these two coordinate systems, it can be shown that the systems $(\varphi_\mathrm{t}^-, \varphi_\mathrm{l}^-)$ and $(\varphi_\mathrm{t}^+, \varphi_\mathrm{l}^+)$ imposed by S^- and S^+, respectively, are related by

$$\begin{pmatrix} \varphi_\mathrm{t}^+ \\ \varphi_\mathrm{l}^+ \end{pmatrix} = M_\mathrm{atom} \cdot \begin{pmatrix} \varphi_\mathrm{t}^- \\ \varphi_\mathrm{l}^- \end{pmatrix} \tag{6}$$

with the integer matrix

$$M_\mathrm{atom} = \begin{pmatrix} 1 & 0 \\ 2 & 1 \end{pmatrix} . \tag{7}$$

This matrix was determined in Ref. 4), but its topological implications were not spelled out in detail. This will be done below.

§4. Invariant tori in the harmonic oscillator

To put the phenomenon discussed in the previous section into a broader context, we will now study a similar, though simpler, situation in which a continuous family

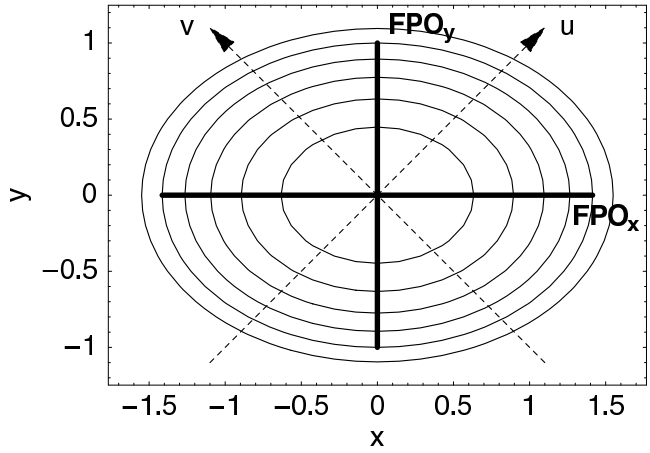

Fig. 2. Illustration of the two-dimensional harmonic oscillator (8) with $\omega_x = 1$ and $\omega_y = 2$. Superimposed over the level lines of the potential energy are the FPOs in the x and y direction for $E = 1$ (thick lines) and the rotated coordinate system (10). Both FPOs intersect the surface of section $v = 0$ (which coincides with the u-axis) at $u = 0$.

of 2-tori are split into two half-families in a Poincaré plot. That example, in which we will be able to carry out all calculations explicitly, is provided by the anisotropic two-dimensional harmonic oscillator described by the Hamiltonian

$$\begin{aligned} H_{\rm osc} &= \frac{1}{2}\left(p_x^2 + p_y^2\right) + \frac{\omega_x^2}{2}x^2 + \frac{\omega_y^2}{2}y^2 \\ &= \omega_x I_x + \omega_y I_y \ , \end{aligned} \tag{8}$$

where in the second line the Hamiltonian has been rewritten in terms of the action variables[13)]

$$I_x = \frac{1}{2}\left(\frac{p_x^2}{\omega_x} + \omega_x x^2\right) \ , \qquad I_y = \frac{1}{2}\left(\frac{p_y^2}{\omega_y} + \omega_y y^2\right) \ . \tag{9}$$

The energy shell for a fixed energy $E > 0$ is foliated into invariant 2-tori that are characterized by fixed values of the actions I_x and I_y related by $\omega_x I_x + \omega_y I_y = E$. In the limit $I_y = 0$, only the motion in the x direction is excited and the tori degenerate into a fundamental periodic orbit FPO$_x$ along the x axis (see Fig. 2). In the opposite limit $I_x = 0$, a second fundamental periodic orbit FPO$_y$ along the y axis is approached. It is therefore clear that there is a single family of invariant tori for which both FPOs act as organizing centers in the sense of §3. Nevertheless, we will see that in a Poincaré surface of section plot this family appears split into two half-families separated by a singularity, and we will find that the topology of the family is characterized by the way in which the half-families are glued together across the singularity.

To find a suitable surface of section that is intersected transversely by both FPOs (so that both FPOs are visible in the plot), we introduce the coordinate system

$$u = \frac{1}{\sqrt{2}}(y + x) \ , \qquad v = \frac{1}{\sqrt{2}}(y - x) \ , \tag{10}$$

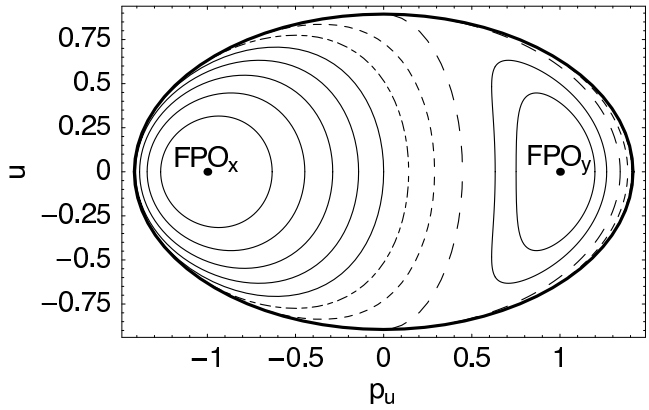

Fig. 3. Poincaré surface of section plot $v = 0$, $p_v \geq 0$ for the two-dimensional harmonic oscillator (8) with $\omega_x = 1$, $\omega_y = 2$ and $E = 1$. Bold line: critical curve $p_v = 0$ where the flow is tangent to the surface of section. Thin lines: invariant tori. For clarity, tori that intersect the critical curve are distinguished by different line types.

which is obtained from the x-y system through a rotation by 45° (see Fig. 2). In these coordinates, we pick the surface of section $v = 0$. For fixed energy E and a fixed starting point $(u,\, p_u)$ on the surface of section, the second component of the momentum is fixed by energy conservation to be

$$p_v = \sqrt{2E - \tfrac{1}{2}\left(\omega_x^2 + \omega_y^2\right) u^2 - p_u^2}\,,$$

where we use the positive square root. For this value to be real, the starting point must be located within the ellipse

$$\tfrac{1}{2}\left(\omega_x^2 + \omega_y^2\right) u^2 + p_u^2 = 2E\,. \tag{11}$$

On the ellipse itself, the velocity transverse to the surface of section is $\dot{v} = p_v = 0$. Thus, on this critical curve the Hamiltonian flow is tangential to the surface. The critical curve itself is not invariant under the flow, which in general leads to discontinuities of the Poincaré map.[14] We avoid discontinuities in this case because the critical curve is the boundary of the surface of section. Nevertheless, the topology of the entire family of invariant tori is not represented faithfully (as, again, it cannot be in a planar plot). Each FPO is surrounded by invariant tori that intersect the surface of section in a closed curve that encloses the FPO. Some tori, however, intersect the critical curve and appear split into two segments, not as a closed curve. Precisely which tori suffer this distortion depends on the choice of the surface of section. Thus, the singularity that splits the family of tori into half-families in the Poincaré plot is here induced by the coordinate system (u, v) used to define the surface of section. It is not a physical singularity of the flow, as it was in the crossed-fields hydrogen atom.

For the harmonic oscillator, it is easy to see how the two half-families of POs must be glued together: In the vicinity of FPO_x, the motion in the x direction is longitudinal, the motion in the y direction is transverse. Conversely, in the neighbourhood of FPO_y, the y motion is longitudinal, the x motion is transverse. The

change of coordinates that maps the longitudinal and transverse modes around FPO_x to those around FPO_y must exchange x and y dynamics and is therefore given by the gluing matrix

$$M_{\mathrm{osc}} = \begin{pmatrix} 0 & 1 \\ 1 & 0 \end{pmatrix} . \tag{12}$$

§5. Lens spaces

The examples described in §§3 and 4 have a similar structure: The energy shell is foliated into families of invariant 2-tori that degenerate into two stable FPOs in two opposite limits. In a Poincaré plot, however, this family appears split into two half-families separated by a singularity. The entire family of tori, including both FPOs, can be obtained by gluing together the two half-families along their boundaries, using an identification of the boundary tori that is given by the gluing matrix M in Eqs. (7) or (12). Because the gluing matrix describes how the tori are to be connected across the singularity, it becomes plausible to regard it as describing a property of the singularity itself, be it the physical singularity of the Coulomb potential in Eq. (7) or the coordinate-induced singularity of the Poincaré map in Eq. (12).

The gluing procedure required here is a well-studied operation. It yields a topological space known as a three-dimensional lens space.[15)–17)] Specifically, if the gluing is carried out with the gluing matrix

$$M = \begin{pmatrix} p & r \\ q & s \end{pmatrix} , \tag{13}$$

where $q > 0$ and $0 \leq p < q$, one obtains the lens space $L_{p/q}$. As discussed in §2, the coordinate-change matrix M is required to satisfy $\det M = ps - qr = \pm 1$, which implies that p and q are coprime. For these spaces, a complete topological classification exists that will be outlined below. It can be used to identify the exact topologies of the families of invariant tori that are present in the examples described above. Important special cases of lens spaces are the following: The space $L_{0/1}$ is homeomorphic to the 3-sphere $\mathcal{S}^3$. The degenerate lens space $L_{1/0}$ where M is the identity matrix is $\mathcal{S}^1 \times \mathcal{S}^2$. The space $L_{1/2}$ is homeomorphic to projective 3-space $\mathbb{RP}^3$, i.e., the set of all straight lines though the origin in $\mathbb{R}^4$. Alternatively, $\mathbb{RP}^3$ can be described as the 3-sphere with antipodal points identified.

To understand the implications of the definition of lens spaces more fully, it is important to notice that the systems of longitudinal and transverse coordinates that the FPOs impose upon the 2-tori are not defined uniquely. Changes in these coordinate systems will lead to changes in the gluing matrix that maps one local coordinate system to the other, so that not all entries of M carry meaningful topological information. Specifically, the local coordinate systems are defined by the conditions that the longitudinal action coordinate I_{l} converges to the action of the FPO as the FPO is approached and the transverse action variable I_{t} tends to zero.[4)] These conditions

leave the freedom to redefine the action variables according to

$$I_\mathrm{t} \mapsto I_\mathrm{t} \,, \qquad I_\mathrm{l} \mapsto I_\mathrm{l} + kI_\mathrm{t} \tag{14}$$

with an arbitrary integer k. Correspondingly, the canonically conjugate angle variables have to be redefined as

$$\varphi_\mathrm{t} \mapsto \varphi_\mathrm{t} - k\varphi_\mathrm{l} \,, \qquad \varphi_\mathrm{l} \mapsto \varphi_\mathrm{l} \tag{15}$$

or

$$\begin{pmatrix} \varphi_\mathrm{t} \\ \varphi_\mathrm{l} \end{pmatrix} \mapsto A_k \cdot \begin{pmatrix} \varphi_\mathrm{t} \\ \varphi_\mathrm{l} \end{pmatrix} \qquad \text{with} \qquad A_k = \begin{pmatrix} 1 & -k \\ 0 & 1 \end{pmatrix} \,. \tag{16}$$

Such redefinitions of the coordinates can be carried out independently around both FPOs before the two halves of the family are glued together. They lead to a change of the gluing matrix given by

$$M \mapsto A_{k'} M A_k^{-1} = \begin{pmatrix} p - k'q & pk - kk'q + r - k's \\ q & s + qk \end{pmatrix} \,. \tag{17}$$

Thus, the entry q is invariant under the coordinate change, and p and s are invariant up to multiples of q, i.e. they are invariant modulo q.

In addition to the coordinate change (14), we are free to change the sign of one of the angle variables in either half-family which amounts to changing the signs in either a row or a column of M. We can use this freedom in the choice of sign and in the choice of k and k' in Eq. (17) to reduce any given gluing matrix M with $q \neq 0$ to a form with $q > 0$ and $0 \leq p < q$, so that the glued family of tori is always homeomorphic to one of the lens spaces $L_{p/q}$ defined above. In the exceptional case that $q = 0$, we must have $p = \pm 1$ and $s = \pm 1$ because $\det M = ps - qr = \pm 1$. We can then reduce M to the identity matrix and obtain the degenerate lens space $L_{1/0}$.

Not all lens spaces obtained in this way are different. We can transform the entry p of the gluing matrix into $q - p$, so that the lens spaces $L_{p/q}$ and $L_{(q-p)/q}$ must be homeomorphic. Moreover, we can obtain the same glued family of tori if we interchange the roles of the two half-families and thereby replace the gluing matrix M by its inverse

$$M^{-1} = \begin{pmatrix} s & -r \\ -q & p \end{pmatrix} \,. \tag{18}$$

After a change of signs, we thus find that $L_{p/q}$ is homeomorphic to $L_{s/q}$. At first sight, this might seem to imply that $L_{p/q}$ and $L_{s/q}$ are homeomorphic for any p, q, s. However, not all values s can occur in the gluing matrix (13) for given p and q, but only those for which there is an integer r such that $\det M = ps - qr = \pm 1$, or, in other words those for which $ps = \pm 1$ modulo q.

In summary, we have found that the lens spaces $L_{p/q}$ and $L_{p'/q}$ are homeomorphic if $p = \pm p'$ modulo q or $pp' = \pm 1$ modulo q. Conversely, it can be shown[15)–17)] that any two homeomorphic lens spaces must satisfy one of these conditions, which gives us a complete topological classification of lens spaces.

§6. Gluing across singularities

With the classification of lens spaces at our disposal, we can use it to identify the topologies of the families of tori encountered in §§3 and 4. Since in both cases the tori foliate the entire energy shell, this is at the same time the topology of the energy shell.

For the harmonic oscillator discussed in §4, the gluing of the two half-families of tori with the gluing matrix M_{osc} in Eq. (12) yields the lens space $L_{0/1}$, which is homeomorphic to the 3-sphere $\mathcal{S}^3$. This result can easily be confirmed by studying the energy shell of the Hamiltonian (8) directly: The equation $H_{\text{osc}} = E$ of the energy shell describes an ellipsoid in phase space, which is topologically equivalent to a sphere. This simple example illustrates that the gluing procedure derived from the study of Poincaré plots and their singularities provides a reliable tool to investigate the topology of the energy shell.

In contrast to the result for the harmonic oscillator, the topology of the energy shell in the crossed-fields hydrogen atom is far from obvious. Using the gluing matrix M_{atom} in Eq. (7) yields the lens space $L_{1/2}$, which is homeomorphic to real projective 3-space $\mathbb{RP}^3$. This remarkable finding implies, in particular, that the energy shell in the planar crossed-fields system is not orientable.

It has been argued above that the gluing matrix should be regarded as a property of the singularity that the gluing has to bridge. If this is correct, the topology found in the crossed-field hydrogen atom should be determined only by the Coulomb singularity, and it should be possible to find the same topology in the field-free hydrogen atom, i.e. the unperturbed planar Kepler problem. That this is indeed the case can be seen if one uses the well known Moser regularization of the Kepler problem,[18] which uses a stereographic projection in momentum space and a rescaling of time to map the planar Kepler problem to the geodesic motion on the 2-sphere, i.e. the dynamics of a free particle that is constrained to move on a sphere. The phase space of this geodesic motion is the tangent bundle of the sphere, the set of all pairs $(\boldsymbol{q}, \boldsymbol{p})$ of 3-dimensional vectors, where $\boldsymbol{q}$ denotes a position on the sphere ($|\boldsymbol{q}| = 1$) and $\boldsymbol{p}$ is a momentum vector perpendicular to $\boldsymbol{q}$. The energy shell in this phase space is given by

$$H_{\text{free}} = \frac{\boldsymbol{p}^2}{2} = E \tag{19}$$

or $|\boldsymbol{p}| = \sqrt{2E}$. If we choose units such that $E = 1/2$, the energy shell consists of all phase space points with $|\boldsymbol{p}| = 1$. This set, which is called the unit tangent bundle of the 2-sphere, is homeomorphic[15] to the projective space $\mathbb{RP}^3$.

Thus, we obtain the same topology from the study of the unperturbed Kepler problem that was found through the study of POs in the crossed-fields system. However, there is a caveat: $\mathbb{RP}^3$ is homeomorphic to the energy shell of the *regularized* Kepler problem. The energy shell of the true, non-regularized Kepler problem is obtained when all phase space points are removed in which the electron is located at the singularity. Because the electron can enter into the singularity from every direction, these points form a circle in phase space. This need to regularize is anal-

ogous to what is found in the harmonic oscillator: In that case, some tori encounter the coordinate-induced singularity of the Poincaré map and are therefore not part of either half-family. Nevertheless, the energy shell contains these tori. In a similar manner, the points in the Coulomb singularity must be included in the energy shell that has the topology described by the gluing procedure.

So far, we have restricted our discussion to systems with two degrees of freedom. The investigations of Ref. 4), by contrast, were focused on invariant tori in a higher-dimensional phase space. In particular, we there identified a second family of invariant 2-tori that do not lie in the 2-dimensional subsystem studied here. Nevertheless, this family is characterized by the same gluing matrix M_{atom}, and we can conclude that it must also be homeomorphic to the projective space $\mathbb{RP}^3$. Because this family is also obtained by gluing across the Coulomb singularity, this observation confirms that the gluing matrix can be regarded as a property of the singularity across which the gluing is carried out.

We have demonstrated in two examples that topological information that can be extracted from periodic orbits in a near-integrable system can lead to a complete topological characterization of families of invariant 2-tori in terms of lens spaces. This approach ties in neatly with the techniques developed in Ref. 4) to study systems with more than two degrees of freedom. It therefore offers a general way to investigate families of invariant 2-tori in higher-dimensional Hamiltonian systems.

Acknowledgements

We are grateful to Alexey Bolsinov for stimulating discussions and a critical reading of the manuscript. This research was partially supported by the US National Science Foundation.

References

1) P. Cvitanović, R. Artuso, R. Mainieri, G. Tanner and G. Vattay, *Chaos: Classical and Quantum*, `ChaosBook.org` (Niels Bohr Institute, Copenhagen, 2005).
2) H. Poincaré, *Les Méthodes Nouvelles de la Méchanique Céleste* (Gauthier-Villars, Paris, 1892).
3) M. C. Gutzwiller, *Chaos in Classical and Quantum Mechanics* (Springer-Verlag, New York, 1990).
4) Stephan Gekle, Jörg Main, Thomas Bartsch and T. Uzer, Phys. Rev. Lett. **97** (2006), 104101; Nonlinear Phenomena in Complex Systems, in press, 2007; Phys. Rev. A **75** (2007), 023406.
5) V. I. Arnold, *Mathematical Methods of Classical Mechanics* (Springer-Verlag, New York, 1989).
6) A. V. Bolsinov and A. T. Fomenko, *Integrable Hamiltonian Systems* (Chapman & Hall/CRC, Boca Raton, Florida, 2004).
7) M. Born, *The Mechanics of the Atom* (Bell, London, 1927).
8) G. D. Birkhoff, Mem. Pont. Acad. Sci. Novi Lyncaei **1** (1935), 85.
9) A. J. Lichtenberg and M. A. Lieberman, *Regular and Chaotic Dynamics* (Springer, New York, 1992).
10) T. Uzer, Physica Scripta **T90** (2001), 176.
11) E. Flöthmann, J. Main and K. H. Welge, J. of Phys. B **27** (1994), 2821.
12) Eugen Flöthmann and Karl H. Welge, Phys. Rev. A **54** (1996), 1884.
13) H. Goldstein, *Classical Mechanics* (Addison-Wesley Publishing Company, Reading, MA, 1965).

14) H. R. Dullin and A. Wittek, J. of Phys. A **28** (1995), 7157.
15) Allen Hatcher, *Algebraic Topology* (Cambridge University Press, Cambridge, 2001).
16) Matthew R. Watkins, *A Short Survey of Lens Spaces* (unpublished). Available online at `www.maths.ex.ac.uk/~mwatkins/lensspaces.pdf` (accessed December 15, 2006), p. 1990.
17) K. Reidemeister, Abh. Math. Sem. Univ. Hamburg **11** (1935), 102.
18) J. Moser, Comments Pure Appl. Math. **23** (1970), 609.